Reprocessing of the COCORP data recorded across the Wichita Mountain uplift and the Anadarko basin in southern Oklahoma

by
W.F. Agena[1], M.W. Lee[1], and J.A. Grow[1]

U.S. Geological Survey
Open-File report 89-357

1 U.S. Geological Survey, MS 960,Box 25046, DFC, Denver, CO 80225

1989

TABLE OF CONTENTS

ILLUSTRATIONS

TABLES

Introduction

In 1979, the Consortium for Continental Reflection Profiling (COCORP) conducted a seismic survey to image a major tectonic feature in the southern midcontinent area of the United States known as the southern Oklahoma aulocogen, which formed during late Pre-Cambrian time (Brewer and others, 1983). Within the aulocogen there is a series of northwest-southeasterly trending faults known as the frontal Wichita Fault system which formed in Pennsylvanian time during a period of significant crustal shortening. During this period the predominantly crystalline rocks of the Wichita Mountains were thrust northeastward over the sedimentary rocks of the Anadarko Basin. Figure 1 shows a map and generalized cross section of the Oklahoma region. The COCORP data were collected in two parts. About 269 linear kilometers of multichannel seismic reflection data were recorded across the Wichita Mountain uplift area in 1979 (Oklahoma Part I). An additional 361 kilometers of data were recorded in 1980 (Oklahoma Part II) extending the survey area into the Anadarko basin. A location map of the COCORP profiles discussed in this report is shown in Figure 2. The map shows the spatial relationship between the surface trace of the seismic profiles and the Mountain View and Meers fault systems. Results from the original processing and interpretations thereof were presented by Brewer and others (1981, 1983). In order to more clearly image the Frontal Wichita Fault system and the southwestern boundary of the Anadarko basin, lines 2, 2A, 5, 5A, 6, and 7 were re-processed, yielding significant improvements in some areas, particularly lines 5A and 2A. The improvements were largely due to crooked line processing, residual statics calculations, and specialized post-stack enhancement techniques developed at the USGS (Lee and others, 1988).

Data Acquisition and Original Processing

All data in this survey were recorded by the Petty-Ray Geophysical Division of Geosource, Inc. under contract to COCORP. An array of 96 acoustic receivers (geophones) grouped 330 feet apart was used to record signals generated by five vibrators located 990 feet away from an end on spread. At each vibrating point (VP), the five vibrators shook for 26 seconds sweeping linearly upward from 8 to 40 Hz. The vibrating points were spaced 990 feet apart, yielding 16-fold common midpoint (CMP) subsurface coverage. For each vibrating point, an MDS-10 system recorded for 42 seconds, sampling at 4 millisecond intervals. The data were recorded on magnetic tape in SEG-B standard format at a density of 1600 bpi. Initial processing of the Oklahoma Part I data set was performed by Petty-Ray in Houston. Figure 3 shows the processing sequence used. Stacking

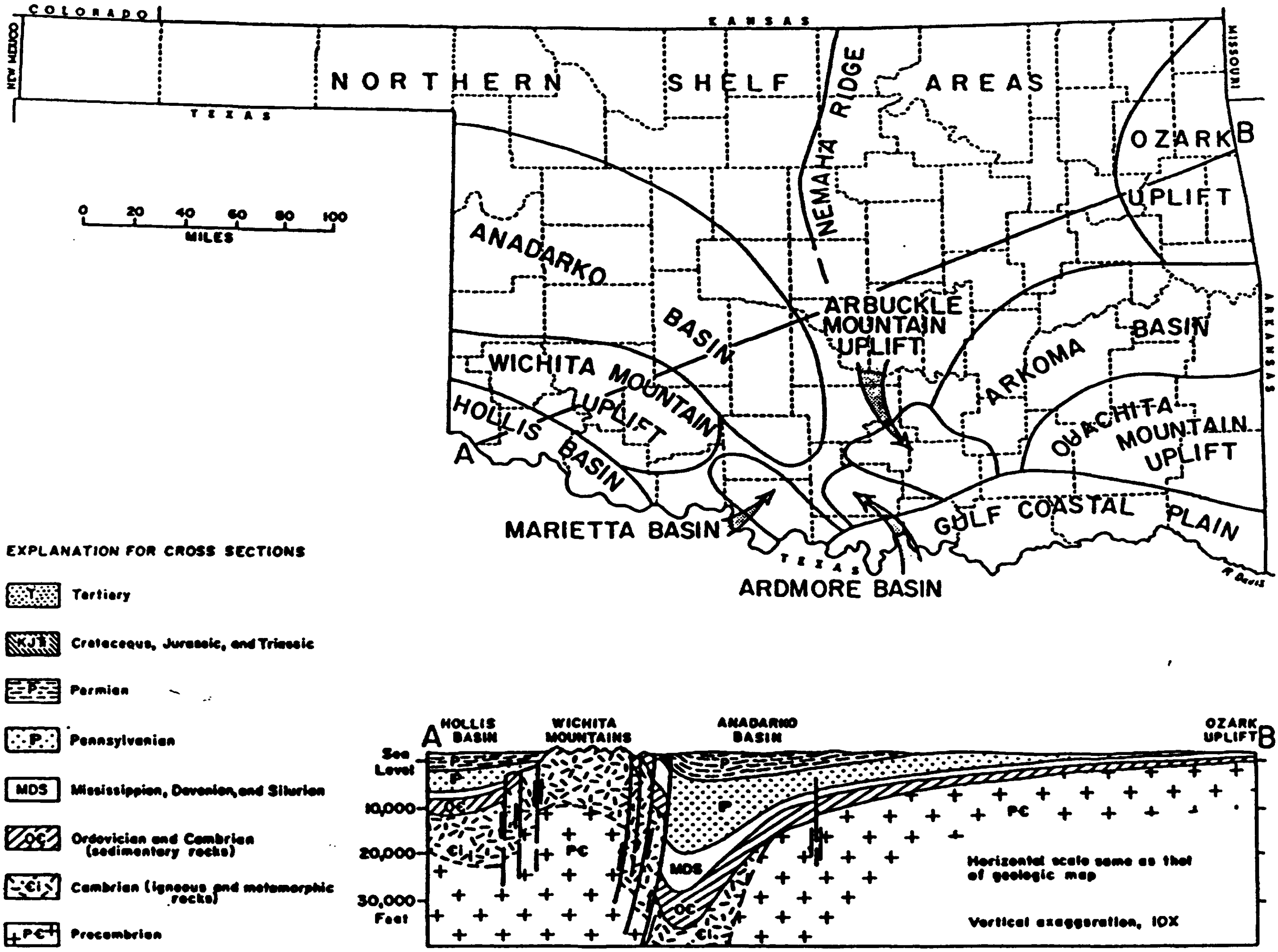

Figure 1 - Generalized map and cross section of the Oklahoma area showing location of basins and other major structural features (from Johnson and Denison, 1973)

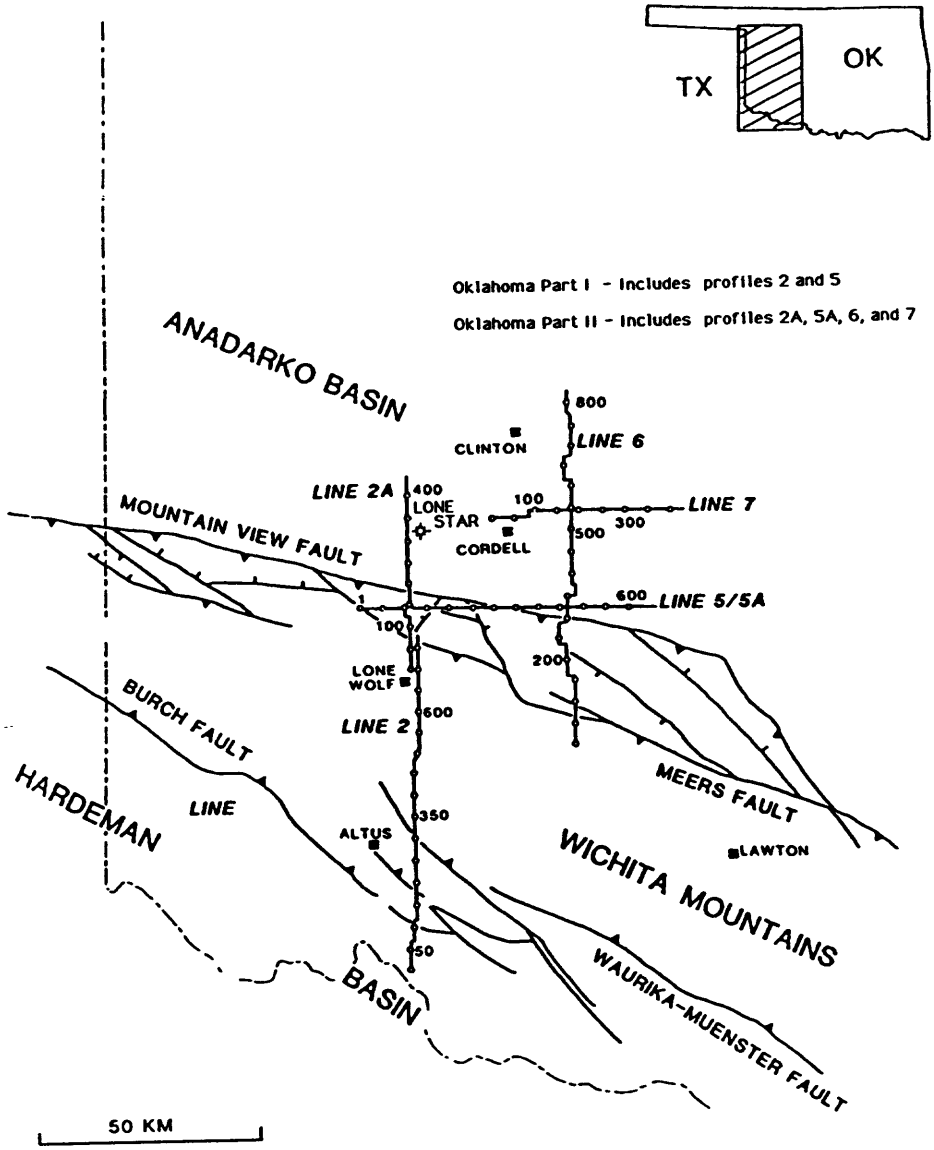

Figure 2 - Generalized map of western Oklahoma showing the locations of lines 2, and 5 from Oklahoma COCORP survey Part I, and lines 2A, 5A, 6, and 7 from COCORP survey Part II.

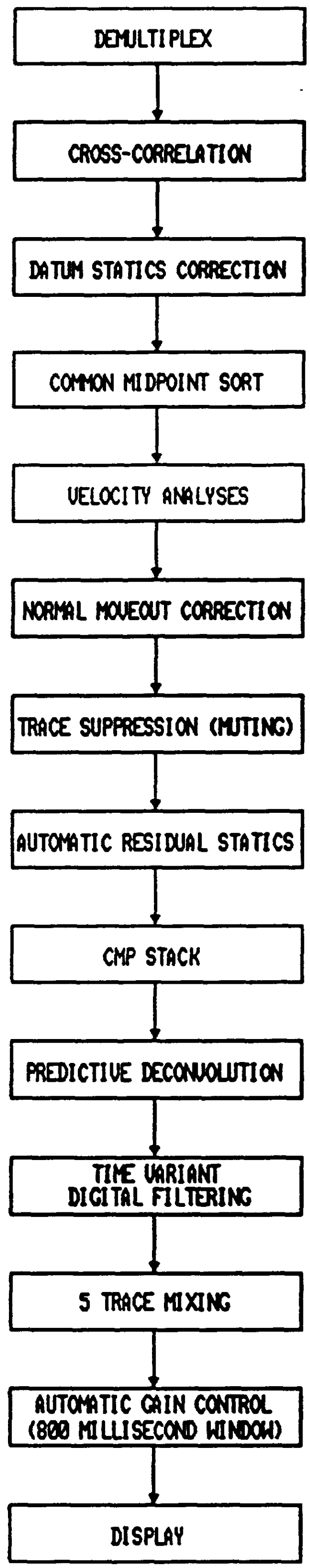

Figure 3 - Flowchart of the original processing sequence used by Cornell University and Petty-Ray Geophysical.

velocities and mute patterns were chosen by personnel from Cornell University's Geological Sciences Department. For the Oklahoma Part II set, processing was done by members of Cornell's Geological Sciences Department on a Megaseis computer using Seiscom Delta processing software. All field data were first demultiplexed into trace sequential order and then cross-correlated with the pilot traces producing record lengths of 16 seconds. The data were then sorted into common midpoint (CMP) order with average of 16-fold coverage, and corrected to a datum plane elevation of 1360 feet. Stacking velocity analyses were then performed to determine proper stacking velocities. After applying normal moveout (NMO) corrections, muting, and applying automatic residual statics, the data were stacked. Post-stack processing included predictive deconvolution, time variant bandpass filtering, and application of an automatic gain control (AGC).

Reprocessing

The lines chosen for USGS reprocessing were purchased directly from the Geological Sciences department of Cornell University. In order to save both time and money, the data purchased were already demultiplexed and cross-correlated. Figure 4 describes the reprocessing sequence used. One noticeable difference between figures 3 and 4 is that we decided not to deconvolve our traces after stack but rather to apply spectral whitening to our data in the frequency domain before stack. An advantage of this method is that we were able to compress the zero-phase Vibroseis wavelets without having to meet the minimum phase assumption needed for spiking deconvolution (Lee 1986). Our next objective was to determine the best way in which to describe a subsurface common midpoint (CMP) line. In deep crustal seismic reflection surveys, array lengths of 1 mile or more are typically found. Designing a survey in a straight line with such large arrays is often a logistical problem. One assumption used in CMP processing is that the midpoints lie directly along the surface survey line. As the survey line bends, this assumption no longer holds true and the surface scatter of the midpoints increases. If the data are processed using a straight line assumption, many traces will be sorted into the wrong CMP gathers. By redefining the CMP locations and limiting the distance offset from each CMP within which a trace can be included, the number of mis-sorted traces can be reduced. This usually produces final stacked sections with a higher signal to noise ratio. Determining the optimal offset distance however, can be difficult. By making the distance too small, only a few traces are left within each CMP resulting in lower redundancy (fold coverage) and correspondingly, stacks with lower signal to noise ratio. Appendix A contains examples describing three geometry

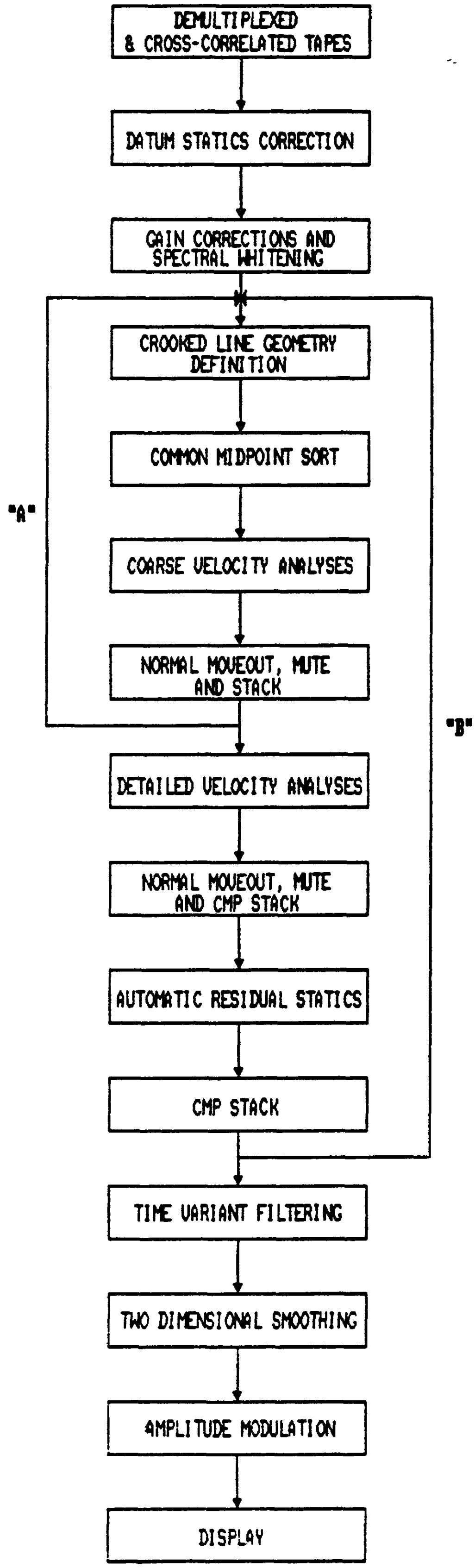

Figure 4 - Flowchart of the reprocessing sequence used by the USGS for COCORP profiles in the Oklahoma region.

configurations with varying degrees of "crookedness" and how the CMP traces can be incorrectly sorted. In crooked line processing, a separate CMP line is defined and traces are assigned to CMPs according to the new surface geometry. Tests were performed on each line to determine the best method of defining a CMP line through the CMP scatter. The three methods used were to define the CMP line: 1) directly beneath the surface line, 2) through the densest portion of the CMP scatters, and 3) through the middle of the scatters. We found that with this particular data set, defining the CMP line through the middle of the scatters produced the best results. An iterative process (loop "A" of figure 4) was used to determine the optimal CMP line and trace offset distances for each line. Usually only two or three iterations were necessary. Another important iterative loop in our processing was the calculation of surface consistent residual statics (loop "B" of figure 4). Different statics windows were tested for each line, producing intermediate stacks of varying quality. Once a stack of acceptable quality was found we continued with post-stack processing which consisted of 1) Time-Variant Bandpass filtering, 2) a two-dimensional smoothing filter, and 3) amplitude modulation. We used a 3 trace by 3 time sample operator for the two-dimensional smoothing. In modulating the trace amplitudes, the input traces were multiplied by their amplitude envelopes raised to the power of .5. A detailed description of both the two-dimensional smoothing filter and the amplitude modulation processes is given by Lee and others (1988). Figure 5(a) shows the northern segment line 6 processed using a CMP line defined directly beneath the surface line, 2 iterations of residual statics, and post-stack enhancement methods. Figure 5(b) shows the same data and processing sequence with the CMP line defined through the middle of the CMP scatters. This method provided noticeable improvement in reflection coherency.

Lines 2 & 2A

Line 2 runs from the Hardeman (Hollis) Basin in the south, past the Burch fault, up through the Wichita Mountains and terminates at the Meers Fault in the north. The poor data quality found on line 2 can be attributed to poor signal penetration within the Wichita Mountain area. Line 2A begins in the Wichita Mountains on the south side of the Meers fault, runs north through the Mountain View fault and terminates in the Anadarko basin. Reprocessing of line 2A resulted in significant improvement in the signal-to-noise ratio and in general coherency of the reflectors. Figures 6 and 7 show line 2A as previously processed and reprocessed, respectively. Figure 8 shows a portion of the previously processed section where line 2A crosses both the Meers fault and the Mountain View fault. In such difficult to process areas, reprocessing still provided improvement as shown in figure 9.

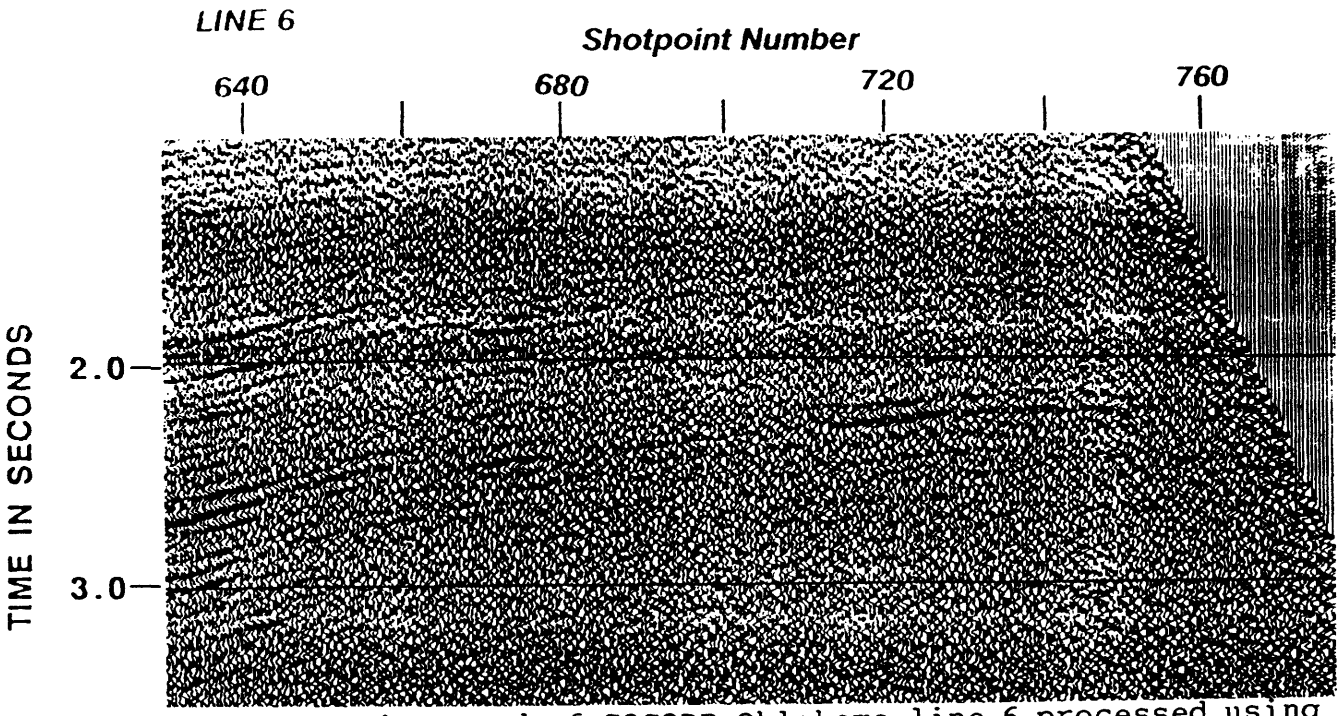

Figure 5a - Northern end of COCORP Oklahoma line 6 processed using a common midpoint(CMP) line defined coincident with the true surface survey line.

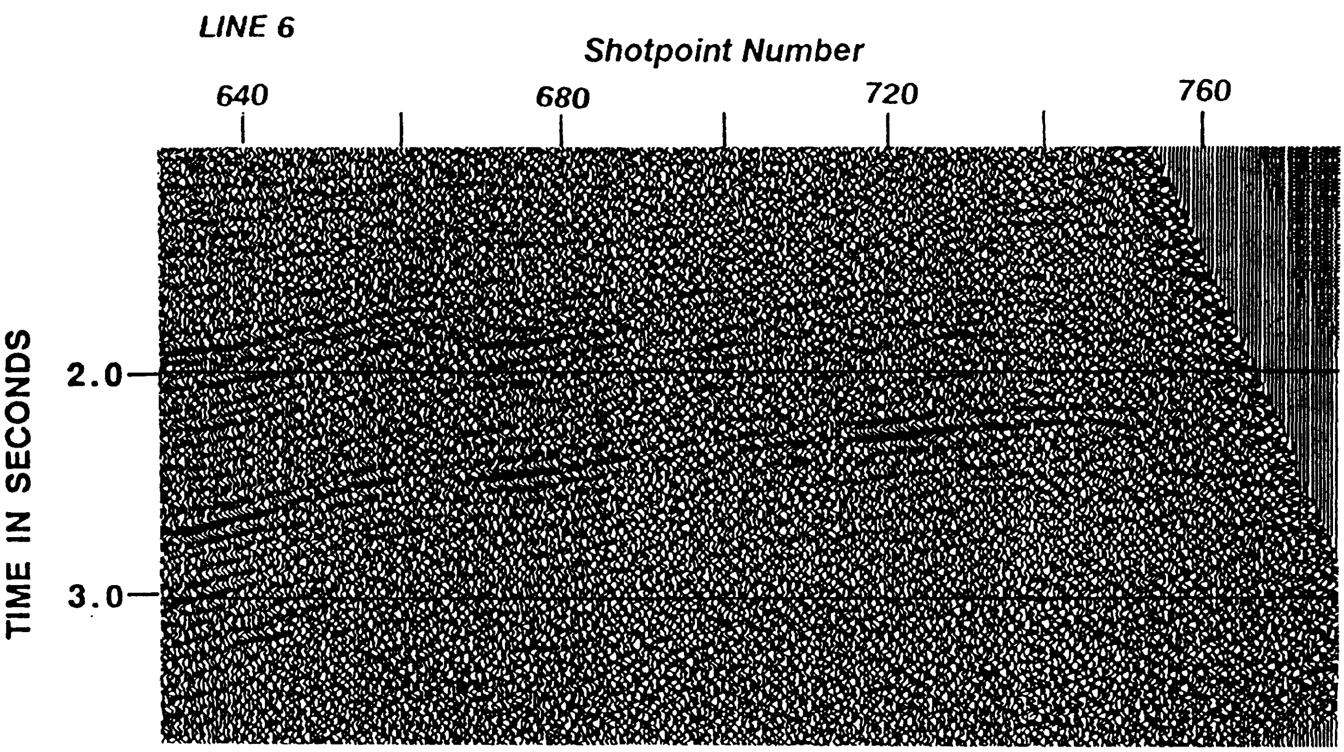

Figure 5b - Same segment of line 6 shown above but with the CMP line defined through the middle of the CMP scatters.

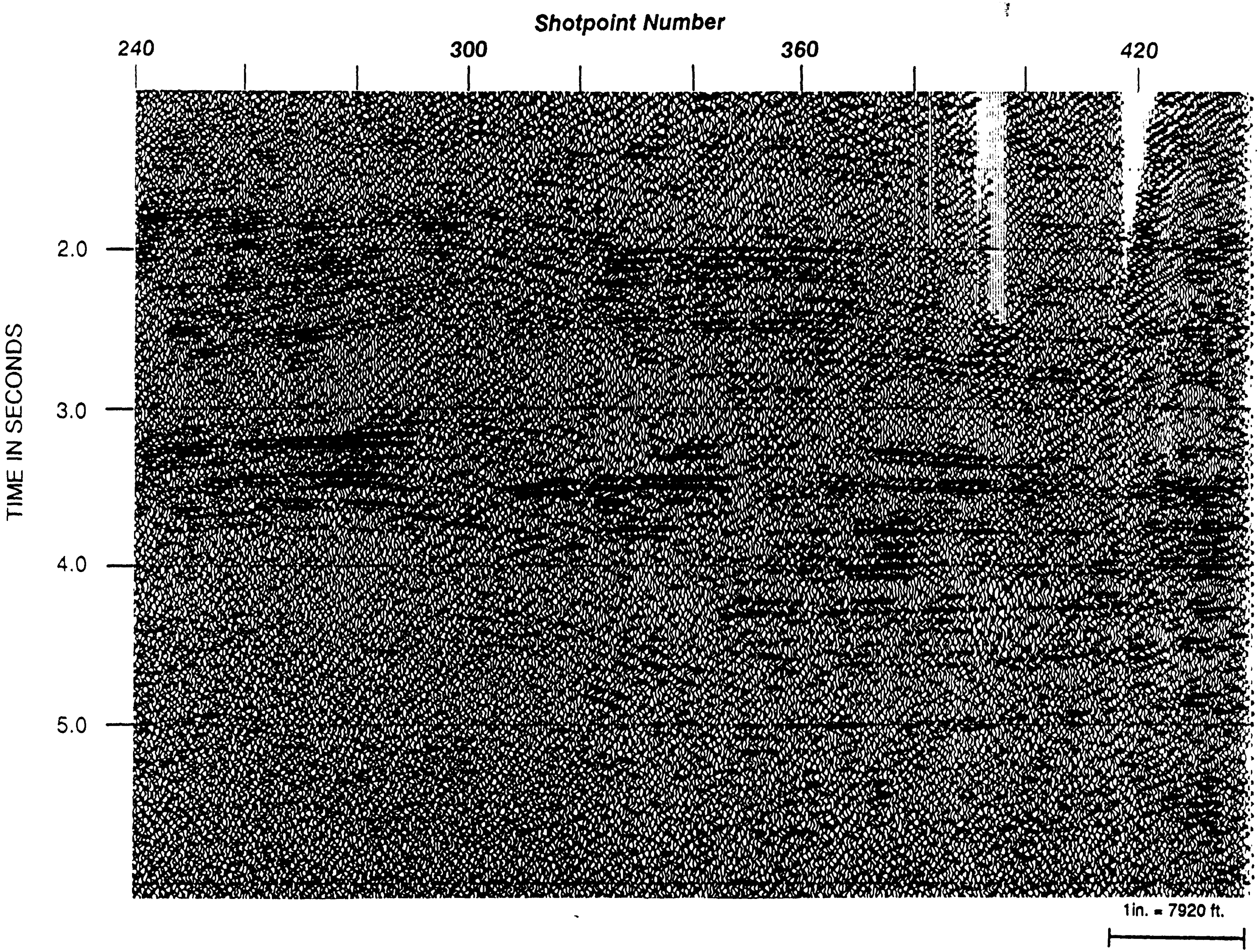

Figure 6 - Segment of COCORP Oklahoma line 2A as originally processed. The segment lies within the Anadarko basin.

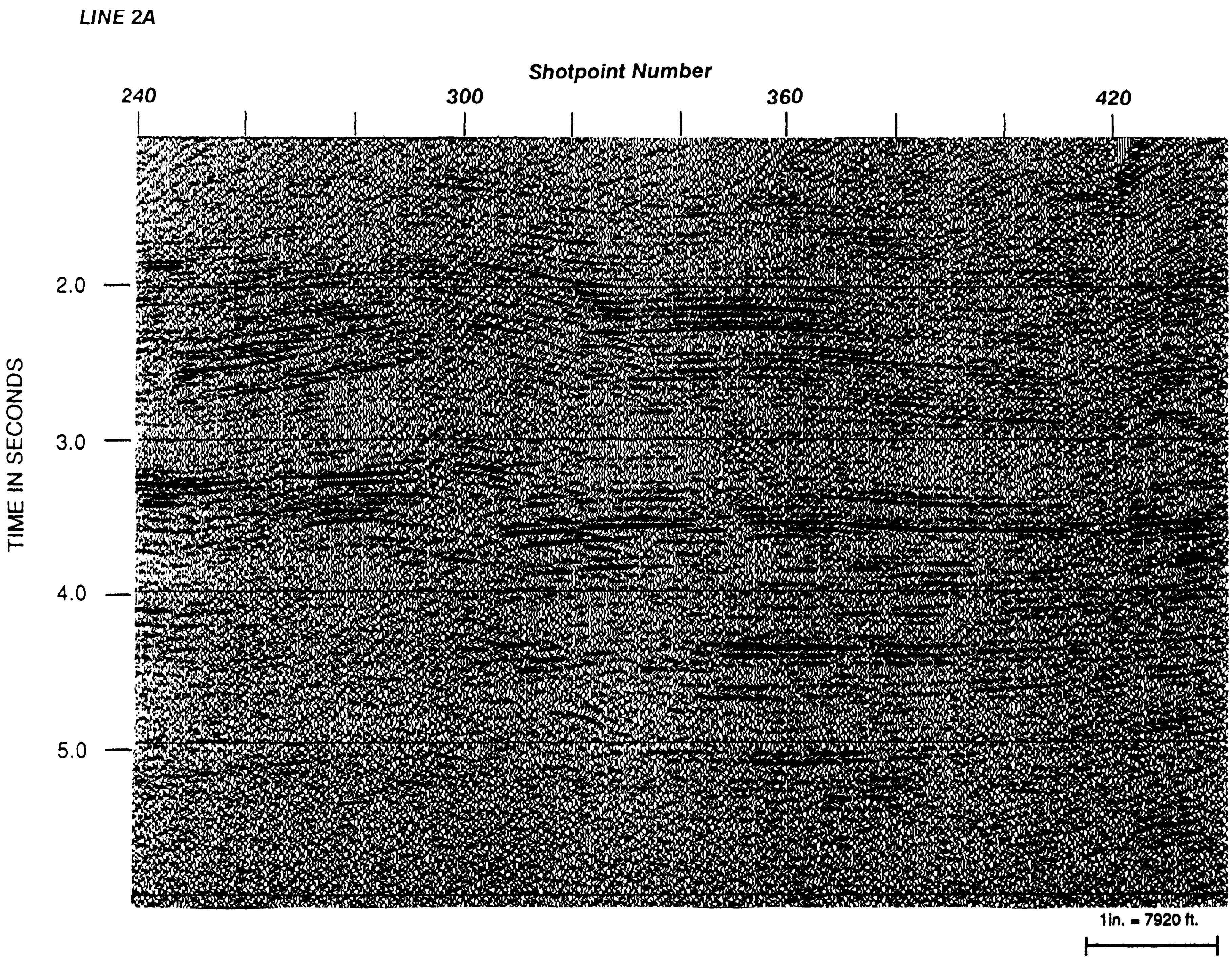

Figure 7 - USGS reprocessed version of segment shown in figure 6

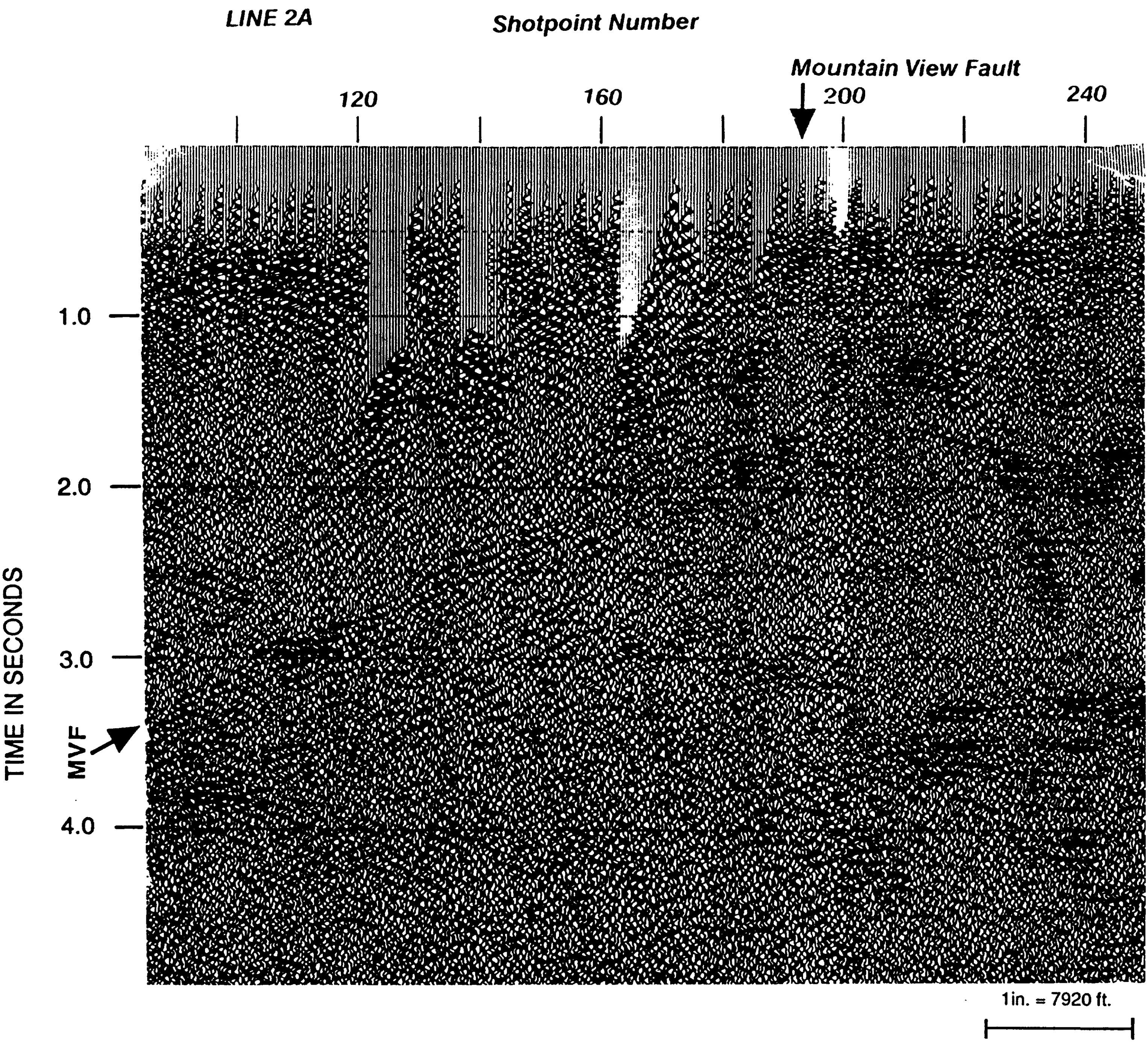

Figure 8 - Segment of COCORP Oklahoma line 2A recorded across the Mountain View fault.

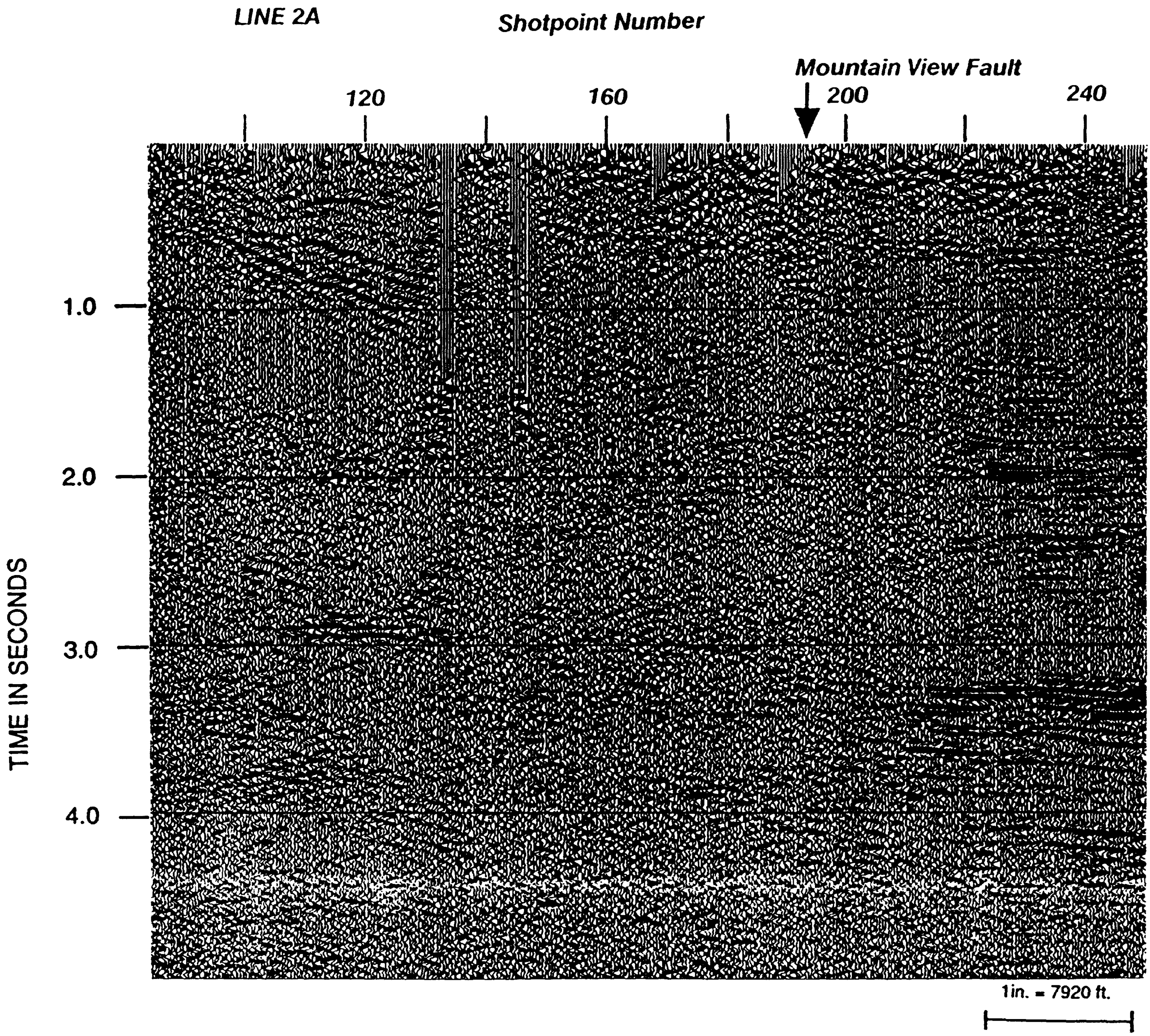

Figure 9 - Reprocessed version of same segment shown in figure 8 .

Lines 5 & 5A

Lines 5 and 5A were shot from west to east, obliquely through the Mountain View fault system. The main Mountain View fault separates the two lines so that line 5 lies almost entirely within the fault system itself and 5A lies almost entirely in the Anadarko basin. Energy scattering within the fault system was probably the cause of poor data on line 5. The most significant results of the reprocessing occur on line 5A as the survey enters the Anadarko basin. A previously processed segment of line 5A directly adjacent to the Meers fault is shown in figure 10. Largely through the use of repeated residual statics tests, and post-stack amplitude modulation, the coherency of the reflectors was greatly improved as seen in figure 11.

Conclusions

COCORP seismic profiles were reprocessed to evaluate the possibility of improved resolution and signal-to-noise ratio over the originally processed profiles, particularly in the vicinity of the Meers and Mountain View faults. We believe that the reprocessing of profiles 2A, 5A, and 6 showed noticeable improvements over the original COCORP profiles, largely due to: 1) Crooked line processing; 2) Better deconvolution (spectral whitening); 3) Improved residual statics calculations; and 4) Post stack enhancement techniques. In addition to the reprocessing of the COCORP profiles, we have inspected industry profiles collected in the last five years to evaluate the current data acquisition techniques which could resolve the structure of the Meers and Mountain View faults. In early 1984, a 1024-channel sign-bit, Vibroseis profile was shot which crosses the eastern end of the Meers fault and achieved spectacular resolution and penetration over both the Meers and Mountain View faults. Industry advances in acquisition techniques allow a much more quantitative analysis of the deformation along the Wichita Mountain front than is possible with the earlier vintage COCORP profiles. While the COCORP profiles have frequently obtained remarkable images of the middle and lower crustal structure, their aquisition configuration (96-channels, 4-millisecond sampling, 16-second records, large group intervals, and long offsets) is not optimized for resolution in the uppermost crust (top 4 seconds). We believe therefore, that it is preferable to reprocess profiles acquired with more optimized field acquisition parameters in order to improve resolution in the deformation zone.

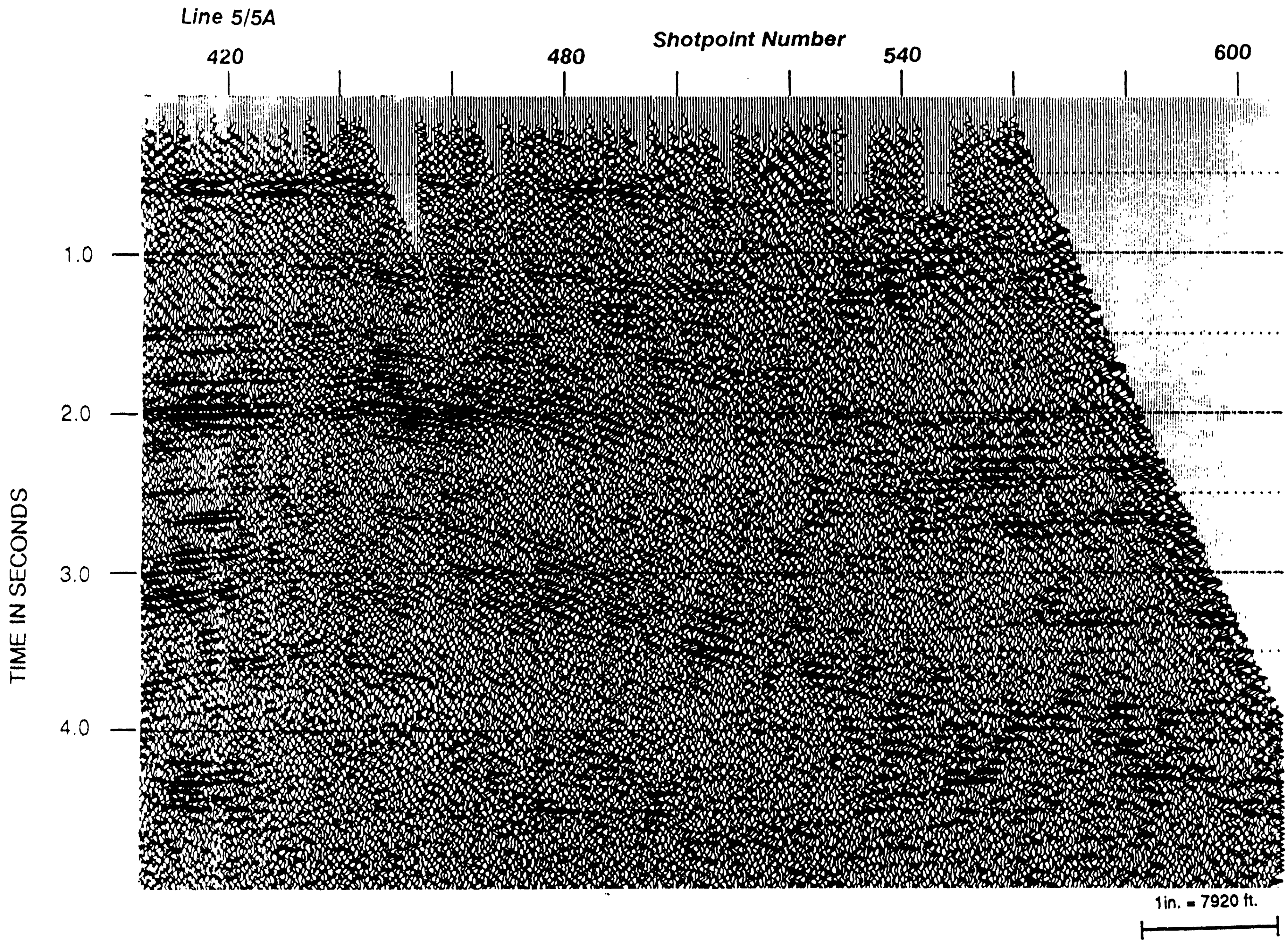

Figure 10 - Segment of line 5A as originally processed.

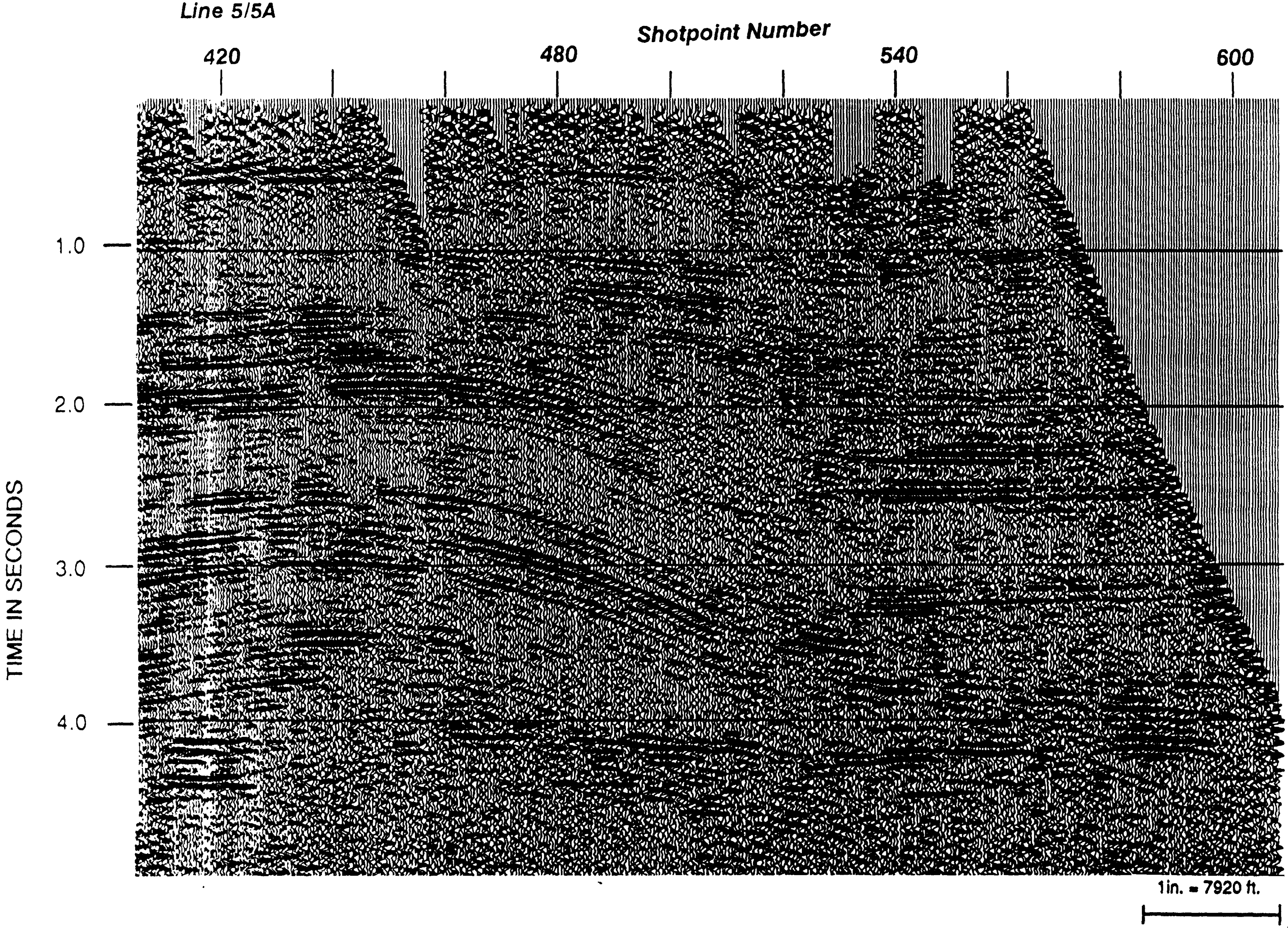

Figure 11 - Reprocessed version of segment shown in figure 10

References

Brewer, J.A., Brown, L.D., Steiner, D., Oliver, J.E., and Kaufman, S., 1981, Proterozoic basin in the southern Midcontinent of the United States revealed by COCORP deep seismic reflection profiling: Geology, v. 9, p. 569-575.

Brewer, J.A., Good, R., Oliver, J.E., Brown, L.D., and Kaufman, S., 1983, COCORP profiling across the Southern Oklahoma aulacogen: Overthrusting of the Wichita Mountains and compression within the Anadarko Basin: Geology, v. 11, p. 109-114.

Johnson, K.S., and Denison, R.E., 1973, Igneous Geology of the Wichita Mountains and Economic Geology of Permian Rocks in Southwest Oklahoma: Guidebook for field trip #6, 1973 GSA meeting, Nov. 9-11, 1973, Dallas, TX, p. 2

Lee, M.W., Agena, W.F., and Hutchinson, D.R., 1988, Processing of the GLIMPCE multichannel Seismic Data: U.S. Geological Survey Open-File Report 88-225.

Lee, M.W., 1986, Spectral Whitening in the Frequency Domain: U.S. Geological Survey Open-File Report 86-108.

Appendix A

Examples of three different geometric configurations for a 10-shot, 4-channel, end-on survey are shown in figure 12. In figure 12(a), a straight line survey is shown. Here the CMP traces lie directly along the survey line. The geometry for the same survey but with with a 45 degree bend is shown in figure 12(b). Notice here that the CMP traces marked by small x's are not all along the survey line. Finally in figure 12(c), we introduce a 90 degree bend. Here again notice the increased scatter among the CMP traces. Table 1 shows CMP stacking charts for the three different geometric configurations. Table 1(a) illustrates the stacking chart for the straight line example. As shown, the first CMP with full fold is CMP 8 located at station 8. This CMP has 4 traces, one from channel 4 of shot 1, a second from channel 3 of shot 2, another from channel 2 of shot 3, and finally one from the first channel of shot 4. In table 1(b), a stacking chart for the line containing the 45 degree bend is shown. With this configuration, channel 1 from shot 9 is incorrectly sorted into CMP 12 instead of CMP 13. A more radical case of misplaced traces is shown in table 1(c), the stacking chart for the line with the 90 degree bend. Here CMP 13 contains no traces to be stacked. By varying the acceptable distance wherein a particular trace can be included within a CMP, the number of mis-sorted traces can be reduced. For example, if in the case of the line with a 90 degree bend, we decide to cut in half the distance within which traces can be accepted, the number of mis-sorted traces is reduced to zero. Also, the CMP located at station 13 that previously contained no traces, now contains one correctly sorted trace. The stacking chart for this example is shown in table 2.

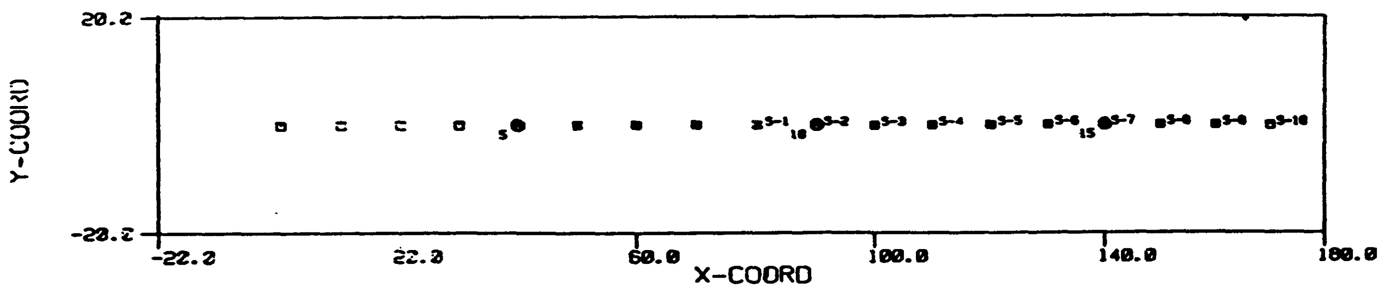

Figure 12a - Map view of a 10-shot straight line survey. Shots are depicted as S-1 through S-10. Small x's mark CMP locations. Squares mark station locations. The first CMP is located beneath station 5

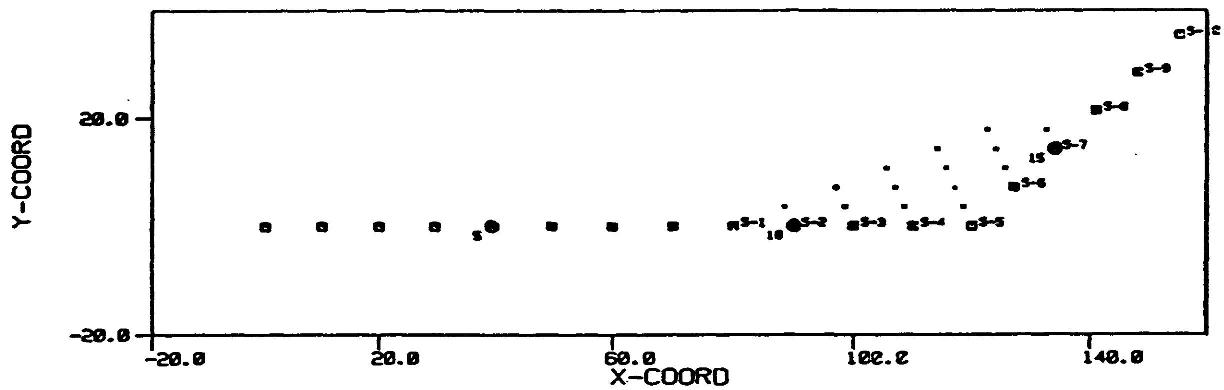

Figure 12b - Map view of a 10-shot survey with a 45-degree bend. Notice the scatter of CMPs.

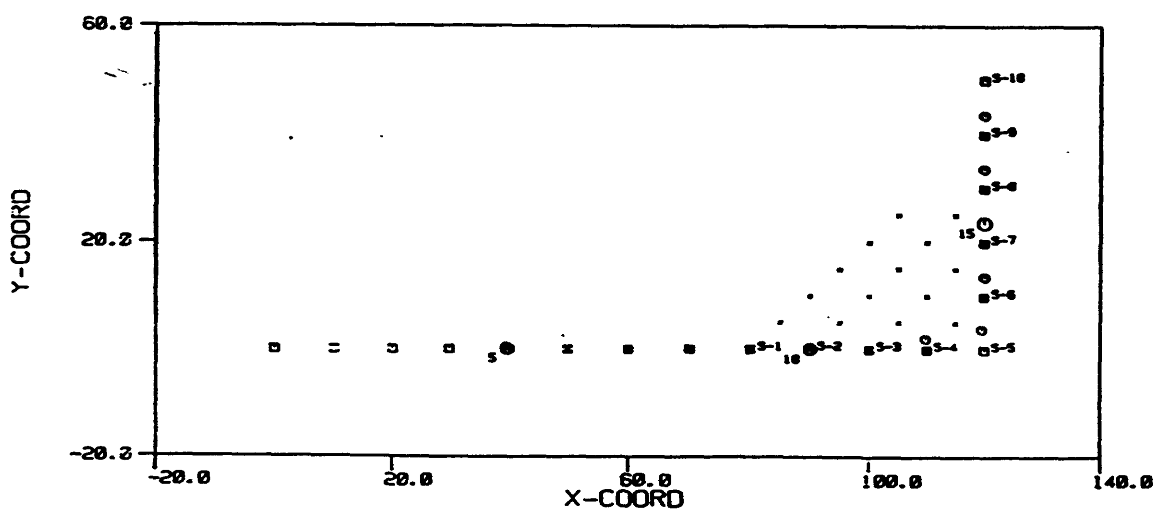

Figure 12c - Map view of a 10-shot survey with a 90-degree bend.

CDP. NO.		5	6	7	8	9	10	11	12	13	14	15	16	17
AT STA.		5	6	7	8	9	10	11	12	13	14	15	16	17
FOLD		1	2	3	4	4	4	4	4	4	4	3	2	1
SHOT	STA.													
1	9	1	2	3	4									
2	10		1	2	3	4								
3	11			1	2	3	4							
4	12				1	2	3	4						
5	13					1	2	3	4					
6	14						1	2	3	4				
7	15							1	2	3	4			
8	16								1	2	3	4		
9	17									1	2	3	4	
10	18										1	2	3	4

Table 1a - Stacking chart of the 10-shot survey shown in figure 12a.

CDP. NO.		5	6	7	8	9	10	11	12	13	14	15	16	17
AT STA.		5	6	7	8	9	10	11	12	13	14	15	16	17
FOLD		1	2	3	4	4	4	4	5	3	4	3	2	1
SHOT	STA.													
1	9	1	2	3	4									
2	10		1	2	3	4								
3	11			1	2	3	4							
4	12				1	2	3	4						
5	13					1	2	3	4					
6	14						1	2	3	4				
7	15							1	2	3	4			
8	16								1	2	3	4		
9	17								1		2	3	4	
10	18										1	2	3	4

Table 1b - Stacking chart of the survey shown in figure 12b. Notice that trace number one of shot nine was incorrectly sorted into CMP 12.

CDP. NO.		5	6	7	8	9	10	11	12	13	14	15	16	17
AT STA.		5	6	7	8	9	10	11	12	0	14	15	16	17
FOLD		1	2	3	4	5	6	6	3	0	2	5	2	1
SHOT	STA.													
1	9	1	2	3	4									
2	10		1	2	3	4								
3	11			1	2	3	4							
4	12				1	2	3	4						
5	13					1	2	3	4					
6	14					1	2	3	4					
7	15						1	2	3		4			
8	16						1	2			3	4		
9	17							1				2 3	4	
10	16											1 2	3	4

Table 1c - Stacking chart of the survey shown in figure 12c. Notice here that all of the traces that should belong to CMP 13 have been incorrectly sorted to the wrong CMP.

CDP. NO.		5	6	7	8	9	10	11	12	13	14	15	16	17
AT STA.		5	6	7	8	9	10	11	12	13	14	15	16	17
FOLD		1	2	3	4	4	3	2	2	1	2	3	2	1
SHOT	STA.													
1	9	1	2	3	4									
2	10		1	2	3	4								
3	11			1	2	3	4							
4	12				1	2	3	4						
5	13					1	2	3	4					
6	14								3	4				
7	15										4			
8	16										3	4		
9	17											3	4	
10	18											2	3	4

Table 2 - Stacking chart of the survey shown in figure 12c but using limited offsets in the sort. Now none of the CMP traces are incorrectly sorted. However, the fold coverage from CMPs 10 through 14 has decreased.